Morphological Shape Comparison Based on Skeleton Representations

Yu. V. Vizilter, S. V. Sidyakin, A. Yu. Rubis, and V. S. Gorbatsevich

State Scientific Research Institute of Aviation Systems, ul. Viktorenko 7, Moscow, 125319 Russia

e-mail: viz@gosniias.ru, sersid@bk.ru, arcelt@mail.ru, gvs@gosniias.ru

Abstract—The concept of a pattern-shape comparison peculiar to the Pyt'ev morphological paradigm is introduced for monotonic morphologies of the Serra type. Morphological skeletons with variable radii (scales) of elements are considered to be analogs of Pyt'ev partitions of a frame into regions with variable brightness. This allows one to construct projections and calculate the morphological coefficients of the correlation.

Keywords: mathematical morphology, image analysis.

DOI: 10.1134/S1054661812020228

1. INTRODUCTION

In [1], it was shown that the Pyt'ev morphological image analysis [2] and the Serra mathematical morphology [3] can be combined within the general formalism of projective mathematical decompositions. The unified formalism allows one to investigate the parallelism of these morphologies and extend the methods and techniques of one morphology to another.

In the paper, a scheme is proposed for a morphological comparison of binary image shapes based on their Skeleton representations. The scheme is in line with the form comparison scheme adopted in the Pyt'ev morphology. A fundamental idea of the proposed approach is that, for the case of binary monotonic morphologies, as constant sets of centers of reference-structuring elements with variable radii (scales), morphological skeletons are analogs of Pyt'ev shapes as constant frame partitions with variable brightness. This idea can be implemented for both discrete and continuous [4] Skeleton representations.

2. SKELETON REPRESENTATIONS OF BINARY FIGURES

In order to discuss skeletons and Skeleton representations of figures in the most general terms, dropping distinctions between different variants of binary morphologies, we introduce the following concepts.

An image space is defined as the set $\mathbf{P}$ of plane points, $\mathbf{P} \subseteq X \times Y$, where X and Y are axes of the rectangular coordinate system.

A binary image is the function

$$B(x, y)\colon X \times Y \longrightarrow \{0, 1\}.$$

A binary figure (pattern) is the set of points

$$\mathbf{B} = \{\mathbf{p} \in \mathbf{P}\colon \mathbf{p} = \langle x, y\rangle, B(x, y) = 1\}.$$

Let there be a set of real numbers $\mathbf{R}$ such that

$$\mathbf{R} = \mathbf{R}^- \cup 0 \cup \mathbf{R}^+, \quad \mathbf{R}^- \in (-\infty, 0),$$

$$\mathbf{R}^+ \in (0, +\infty), \quad \mathbf{R}^- \neq \varnothing, \quad \mathbf{R}^+ \neq \varnothing.$$

In addition, let there be a set of figures $G(\mathbf{R}) = \{\mathbf{G}(r), r \in \mathbf{R}\}$, $\mathbf{G}(\mathbf{R}) \subseteq \mathbf{P}$, which is completely ordered by the strict inclusion relation "$\subset$" and is parametrized by scalars of $\mathbf{R}$ in the sense that there is a biunique correspondence between them and

$$\forall r < 0\colon \mathbf{G}(r) = \varnothing, \quad \mathbf{G}(0) = \langle 0, 0\rangle,$$

$$\mathbf{G}(\sup(\mathbf{R})) = \mathbf{P},$$

$$\forall r, t \in \mathbf{R}\colon t < r \Leftrightarrow \mathbf{G}(t) \subset \mathbf{G}(r).$$

In what follows, the ordered set $\mathbf{G}(\mathbf{R})$ is a basic structuring sequence, its elements $\mathbf{G}(r)$ are basic structuring elements, and the corresponding values of the scalar r are characteristic of the dimension or scale of basic structuring elements. A point $\mathbf{G}(0) = \langle 0, 0\rangle$ is called a center of a basic structuring element, since $\forall r > 0\colon \mathbf{G}(0) \subset \mathbf{G}(r)$.

The shift in figure $\mathbf{B}$ within space $\mathbf{P}$ on the vector $\mathbf{p} = \langle x, y\rangle \in \mathbf{P}$ will be represented by

$$\mathbf{B}(\mathbf{p}) = \{\langle x_b + x, y_b + y\rangle\colon \langle x_b, y_b\rangle \in \mathbf{B}\}.$$

Thus, $\mathbf{B}(\langle 0, 0\rangle) = \mathbf{B}$. The shift operator applied to elements of the basic sequence is conveniently denoted using the additional parameter

$$\mathbf{G}(r)(\mathbf{p}) = \mathbf{G}(\mathbf{p}, r), \mathbf{p} \in \mathbf{P}, \quad r \in \mathbf{R}.$$

Hence, the set $\mathbf{G}(\mathbf{P}, \mathbf{R}) = \{\mathbf{G}(\mathbf{p}, r), p \in \mathbf{P}, r \in \mathbf{R}\}$ is a complete basis of the morphological decomposition [1], i.e., any figure A can be represented as

$$\mathbf{A} = \cup_{p \in \mathbf{P}} \cup_{r \in \mathbf{R}} \{\mathbf{G}(\mathbf{p}, r)\colon \mathbf{G}(\mathbf{p}, r) \subseteq \mathbf{A}\}.$$

Received May 4, 2011

The maximal constituent element of the figure **A** will be called the basic element $\mathbf{G}(\mathbf{p}, r)$, for which the following conditions are fulfilled:

$$1)\ \mathbf{G}(\mathbf{p}, r) \subseteq \mathbf{A},$$

$$2)\ !\exists \mathbf{q} \in \mathbf{P},\quad t \in \mathbf{R},\quad \mathbf{G}(\mathbf{p}, r) \subset \mathbf{G}(\mathbf{q}, t) \subseteq \mathbf{A}.$$

A skeleton of the figure will be called a set of centers of its maximal constituent elements

$$\mathbf{S}(\mathbf{A}) = \{\mathbf{p}: \mathbf{G}(\mathbf{p}, r) \subseteq \mathbf{A},$$

$$!\exists \mathbf{q} \in \mathbf{P},\quad t \in \mathbf{R},\quad \mathbf{G}(\mathbf{p}, r) \subset \mathbf{G}(\mathbf{q}, t) \subseteq \mathbf{A}\}.$$

A radial or distant function of the pattern **A** will be called a scalar function

$$r_A(\mathbf{p}) = \max_{r \in \mathbf{R}}\{r: \mathbf{G}(\mathbf{p}, r) \subseteq \mathbf{A}\}. \quad (1)$$

This allows one to define the Skeleton representation as the set of pairs

$$\mathbf{SR}(\mathbf{A}) = \{\langle \mathbf{p}, r_{\mathbf{A}}(\mathbf{p})\rangle: \mathbf{p} \in \mathbf{S}(\mathbf{A})\}.$$

This description involves all data on the figure shape required for the reconstruction as follows:

$$\mathbf{A} = \cup_{\langle \mathbf{p}, r\rangle \in \mathbf{SR}(\mathbf{A})}\{\mathbf{G}(\mathbf{p}, r)\}.$$

3. SKELETON SHAPE DESCRIPTION AND MORPHOLOGICAL SHAPE COMPARISON

Now, let us consider pattern **B**, for which it is required to compare its shape with the shape of the pattern **A**. Using the radial function (1), one can determine the morphological projection of the binary pattern **B** on the shape of pattern **A** as follows:

$$\Pr(\mathbf{B}, \mathbf{A}) = \cup_{\mathbf{p} \in \mathbf{S}(\mathbf{A})}\{\mathbf{G}(\mathbf{p}, r_{\mathbf{B}}(\mathbf{p}))\}. \quad (2)$$

It is easy to verify that the following basic properties, which hold for morphological projections defined by expression (2):

$$\begin{aligned} &1)\ \Pr(\Pr(\mathbf{B}, \mathbf{A}), \mathbf{A}) = \Pr(\mathbf{B}, \mathbf{A});\\ &2)\ \Pr(\mathbf{A}, \mathbf{A}) = \cup_{p \in \mathbf{S}(\mathbf{A})}\{\mathbf{G}(\mathbf{p}, d_{\mathbf{B}}(\mathbf{A}))\} = \mathbf{A};\\ &3)\ \Pr(\mathbf{B}, \mathbf{A}) \subseteq \mathbf{B};\\ &4)\ \mathbf{C} \subseteq \mathbf{B} \Rightarrow \Pr(\mathbf{C}, \mathbf{A}) \subseteq \Pr(\mathbf{B}, \mathbf{A}). \end{aligned} \quad (3)$$

The first expression shows the algebraic projectivity of this operation. The second expression indicates that the projection of the pattern on the shape of the same pattern do not distort it. The third expression suggests that the projection always belong to the pattern being projected. The fourth expression shows that the projection preserves the inclusion. Thus, reductive projective operator (3) that preserves inclusion is a morphological open-type filter according to the Serra terminology.

It follows from the third expression in (3) that

$$\|\Pr(\mathbf{B}, \mathbf{A})\| \le |\mathbf{B}|,$$

which allows one to determine the Pyt'ev morphological correlation coefficient normalized on the interval [0, 1] as follows:

$$K_M(\mathbf{B}, \mathbf{A}) = \|\Pr(\mathbf{B}, \mathbf{A})\|/\|\mathbf{B}\|. \quad (4)$$

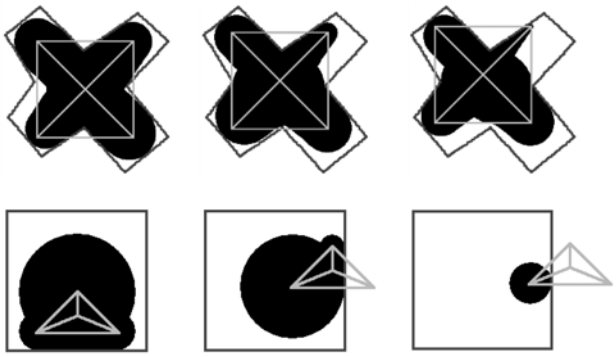

Fig. 1. Examples of projecting figure on shape.

A set of figures invariant to the projection on the shape **A** will be called a model set or a set of figures of shape **A**

$$\mathbf{M}_{\mathbf{A}} = \{\mathbf{B} \subseteq \mathbf{P}: \Pr(\mathbf{B}, \mathbf{A}) = \mathbf{B}\}.$$

The morphological correlation coefficient (4) estimates the degree of proximity of the figure **B** to the model set of the figure **A**; at that,

$$K_M(\mathbf{B}, \mathbf{A}) = 1 \Leftrightarrow \mathbf{B} \in \mathbf{M}_{\mathbf{A}}.$$

In other words, the morphological correlation coefficient estimates the degree of similarity of the shapes of figures **A** and **B**.

The outlined idea of constructing the morphological projection of a binary figure on the shape of another binary figure is illustrated in Fig. 1, where contours of reference and projected figures are shown. The skeleton is traditionally constructed based on the disk-structuring element.

The framework of the Pyt'ev morphological shape comparison is thus proved to extend completely to the case of binary monotonic morphologies. Note that morphological concepts described in this section can be equally applied to discrete and continuous morphological systems, as well as to systems with finite-dimensional and infinite-dimensional basis of the morphological decomposition. Moreover, the concept of a binary figure shape as a Skeleton representation with a variable scale is constructed based on the arbitrary sequence of embedded structuring elements, as well as independent of either the particular selection of the structuring element type or the scaling method. Furthermore, all of the introduced concepts can easily be generalized as they are, on one hand, to the one-dimensional case (binary morphology on a straight line) and, on the other hand, to the case of a higher dimension (half-tone morphology, three-dimensional morphology, etc.) if the shadows under the functions defined in the n-dimensional space are considered as binary patterns (figures) in the space of order $n + 1$.

However, the cost of universality in such a general approach is that the skeleton of the binary figure is an abstract, unordered set of points rather than a continuous planar graph, as is required by our geometric intuition and the established scientific tradition.

In the following subsection, the introduced concepts are concretized for the case of the continuous binary monotonic morphology and it is shown that, in such a statement, Skeleton representations of all obtained projections, as well as skeletons of original figures, will be continuous and piecewise smooth.

3.1. Shape Comparison Based on Skeleton Descriptions with Connections

Let us refer to a free morphological model as a description of the figure shape of the following type

$$\mathbf{M}(\mathbf{A}, \sigma) = \cup_{\mathbf{p} \in \mathbf{S(A)}}\{\mathbf{G}(\mathbf{p}, \sigma(\mathbf{p}))\}, \sigma(\mathbf{p}) \in \Sigma,$$

where $\sigma(\mathbf{p})$ is the arbitrary function (single-valued transformation) from $\mathbf{S(A)}$ to $\mathbf{R}$, and Σ is a certain set of these functions. The set of figures that can be obtained from the skeleton description of $\mathbf{A}$ by changing the radial function is conveniently denoted by

$$\mathbf{M}(\mathbf{A}, \Sigma) = \{\mathbf{M}(\mathbf{A}, \sigma), \sigma \in \Sigma\}.$$

Taking this into account, the morphological projection (2) is the solution to the following optimization problem:

$$\Pr(\mathbf{B}, \mathbf{A}) = \arg\max_{\mathbf{U} \in \mathbf{M}(\mathbf{A}, \Sigma)}\{\|\mathbf{U}\|: \mathbf{U} \subseteq \mathbf{B}\}. \quad (5)$$

Considering that $\mathbf{M}(\mathbf{A}, \sigma) \subseteq \mathbf{B} \Rightarrow \sigma(\mathbf{p}) \le r_{\mathbf{B}}(\mathbf{p})$, the solution of problem (5) can always be represented in the following shape

$$\begin{gathered}\Pr(\mathbf{B}, \mathbf{A}) = \mathbf{M}(\mathbf{A}, \sigma_{\mathbf{B}}),\\ \sigma_{\mathbf{B}}(\mathbf{p}) = \arg\max_{\sigma(p) \in \Sigma}\{\|\mathbf{M}(\mathbf{A}, \sigma)\|: \\ \sigma(\mathbf{p}) \le r_{\mathbf{B}}(\mathbf{p}), \mathbf{p} \in \mathbf{S(A)}\}.\end{gathered} \quad (6)$$

In the case when there are no prior restrictions on Σ, the solution of problem (6) is in the above-mentioned simplest shape

$$\sigma_{\mathbf{B}}(\mathbf{p}) = r_{\mathbf{B}}(\mathbf{p}).$$

Note that $\sigma(\mathbf{p})$ by no means depends on $r_{\mathbf{A}}(\mathbf{p})$. In the left side of Fig. 1, it is demonstrated that this freedom results from connections and prior restrictions. The projection shape depends on the projected figure and bears little resemblance to the reference shape from the intuitive viewpoint. To remedy this, it is required to limit in one some way the class of functions Σ, wherein the solution to problem (6) is sought.

Let us consider the following quite strong, but intuitively acceptable assumption. If values of the radial function of two points coincide in the original Skeleton representation (that is, the thickness of the figure in these two points is uniform), then they should also coincide in the projection as follows:

$$\forall \mathbf{p}, \mathbf{q} \in \mathbf{S(A)}: r_{\mathbf{A}}(\mathbf{p}) = r_{\mathbf{A}}(\mathbf{q}) \Rightarrow \sigma_{\mathbf{B}}(\mathbf{p}) = \sigma_{\mathbf{B}}(\mathbf{q}).$$

In this case, the transformation of the figure can always be described by the following functional dependence:

$$\sigma(\mathbf{p}) = f(r_{\mathbf{A}}(\mathbf{p})). \quad (7)$$

Let $f \in \mathrm{F}$, where F is a certain prescribed class of functions. Then, the class of functions Σ in problem (6) is uniquely defined as $\Sigma(\mathbf{A}, \mathrm{F})$.

The simplest model of this type involves the expansion/contraction of the figure by adding an arbitrary constant to the radial function as follows:

$$\begin{gathered}f(t) = t + b, \quad \sigma_{\mathbf{B}}(\mathbf{p}) = r_{\mathbf{A}}(\mathbf{p}) + b_{\mathbf{B}},\\ b_{\mathbf{B}} = \min_{\mathbf{p} \in \mathbf{S(A)}}\{r_{\mathbf{B}}(\mathbf{p}) - r_{\mathbf{A}}(\mathbf{p})\}.\end{gathered} \quad (8)$$

Indeed, in the case of a continuous morphology with a circular structuring element, it can easily be shown that adding the positive constant b to all values of the radial function of the original skeleton implements the Serra function of the expansion (dilatation) of the original figure by the disk structuring element of radius b as follows:

$$\begin{gathered}\cup_{\mathbf{p} \in \mathbf{S(A)}}\{\mathbf{D}(\mathbf{p}, r_{\mathbf{A}}(\mathbf{p}) + b)\}\\ = \cup_{\mathbf{p} \in \mathbf{A}}\mathbf{D}(\mathbf{p}, b) = \mathbf{A} \oplus \mathbf{D}(b).\end{gathered}$$

Conversely, adding the negative constant b to values of the radial function implements in shape (8) the Serra contraction (erosion) function with the disk element of radius b as follows:

$$\begin{gathered}\cup_{\mathbf{p} \in \mathbf{S(A)}}\{\mathbf{D}(\mathbf{p}, r_{\mathbf{A}}(\mathbf{p}) - b)\}\\ = \cup\{\mathbf{p}: \mathbf{D}(\mathbf{p}, b) \subseteq \mathbf{A}\} = \mathbf{A} \ominus \mathbf{D}(b).\end{gathered}$$

Let us introduce the following universal designation:

$$\begin{gathered}\mathbf{A} \oplus b = \{\mathbf{A} \oplus \mathbf{D}(b): b \ge 0;\\ \mathbf{A} \ominus \mathbf{D}(-b): b < 0\}.\end{gathered} \quad (9)$$

Then, the set of figures of the same shape is

$$\mathbf{M}(\mathbf{A}, b) = \{\mathbf{A} \oplus b, b \in \mathbf{R}\}$$

and the solution to problem (6) with allowance for (9) can be written as

$$\begin{gathered}\Pr(\mathbf{B}, \mathbf{M}(\mathbf{A}, b)) = \mathbf{A} \oplus b_{\mathbf{B}},\\ b_{\mathbf{B}} = \arg\max_{b \in \mathbf{R}}\{\|\mathbf{A} \oplus b\|: (\mathbf{A} \oplus b) \subseteq \mathbf{B}\}.\end{gathered}$$

Examples of these operations are given in Fig. 2.

Another parametrized set of shapes $\mathbf{M}(\mathbf{A}, a)$ can be generated using the model of thinning/thickening the figure (Fig. 3):

$$\begin{gathered}f(t) = at, \quad \sigma_{\mathbf{B}}(\mathbf{p}) = a_{\mathbf{B}} \cdot r_{\mathbf{A}}(\mathbf{p}),\\ a_{\mathbf{B}} = \min_{\mathbf{p} \in \mathbf{S(A)}}\{r_{\mathbf{B}}(\mathbf{p})/r_{\mathbf{A}}(\mathbf{p})\}.\end{gathered}$$

The thickening of the figure takes place for $a > 1$, while thinning takes place for $a < 1$. The choice of $a < 0$ results in $\mathbf{M}(\mathbf{A}, \sigma) = \varnothing$. Let us introduce the corresponding designation as follows:

$$\mathbf{A} \otimes a = \cup_{\mathbf{p} \in \mathbf{S(A)}}\{\mathbf{D}(\mathbf{p}, ar_{\mathbf{A}}(\mathbf{p}))\}.$$

Then, the solution of problem (6) will take the following shape

$$\Pr(\mathbf{B}, \mathbf{M}(\mathbf{A}, a)) = \mathbf{A} \otimes a_{\mathbf{B}},$$

$$a_{\mathbf{B}} = \arg\max_{a \in \mathbf{R}} \{ \|\mathbf{A} \otimes a\| : (\mathbf{A} \otimes a) \subseteq \mathbf{B} \}.$$

It is possible to consider other more complex classes of radial function transformations.

By and large, these morphological models can naturally be called models with fixed connections or models with restrictions. These models formalize various intuitive ideas about the degree of variability of the shape of the figure in practical problems. It is significant that, in all of these cases, the projectivity of morphological operators of the shape comparison takes place, and morphological correlation coefficients can be calculated.

3.2. Shape Comparison Invariant to Image Shift

All of the above operators of projecting a figure on the shape of another figure were noninvariant to the shift of the projected figure with respect to the reference shape. However, secondary invariant operators can easily be defined based on noninvariant operators.

Let there be the model set $\mathbf{M}(\mathbf{A}, \Sigma)$, and the corresponding projection operator $\Pr(\mathbf{B}, \mathbf{M}(\mathbf{A}, \Sigma))$ be defined. Then, the shift-invariant shape projector can be defined as an operator choosing an inscribed pattern with the maximal norm within a given model class as follows:

$$\mathrm{PR}(\mathbf{B}, \mathbf{M}(\mathbf{A}, \Sigma)) = \arg\max_{\mathbf{p} \in \mathbf{P}} \|\Pr(\mathbf{B}, \mathbf{M}(\mathbf{A}(\mathbf{p}), \Sigma))\|.$$

Examples of these invariant projections for different projector types are given in Fig. 4. In Fig. 4, the invariant projection of a rectangle on the free triangle shape is shown on the left, the invariant projection on the class of expansion/contraction shapes is presented in the center, and the invariant projection on the class of thinning/thickening shapes is presented on the right.

4. MORPHOLOGICAL PROJECTION IN CONTINUOUS BINARY MORPHOLOGY

Following the description of the continuous binary morphology [4], we adopt following definitions. A Jordan curve is a continuous injective circle pattern with regard to its mapping in the Euclidean plane $\mathbf{P} = \mathbf{R}^2$, where $\mathbf{R}$ is the set of real numbers. An important point is that the Jordan curve has no self-intersections. The figure is a connected closed domain of a plane restricted by a finite number of nonintersecting Jordan curves. Let $\mathbf{P}$ be the Euclidean plane with the corresponding distance $d(\mathbf{p}, \mathbf{q})$, $\mathbf{p}, \mathbf{q} \in \mathbf{P}$. Then, the boundary of the figure $\mathbf{A}$ is defined as the set of points

$$\partial\mathbf{A} = \{\mathbf{p}: \mathbf{p} \in \mathbf{P}, \forall r > 0, \mathbf{D}(\mathbf{p}, r) \cap \mathbf{A} \neq \varnothing,$$

$$\mathbf{D}(\mathbf{p}, r) \cap \mathbf{A}^{\mathbf{C}} \neq \varnothing\},$$

where $\mathbf{A}^{\mathbf{C}} = \mathbf{P} \backslash \mathbf{A}$ is the complement or background of the figure $\mathbf{A}$, and $\mathbf{D}(\mathbf{p}, r)$ is the open circle of radius r with its center at $\mathbf{p}$ determined by the following expression:

$$\mathbf{D}(\mathbf{p}, r) = \{\mathbf{q}: \mathbf{q} \in \mathbf{P}, d(\mathbf{p}, \mathbf{q}) < r \in R\}.$$

The circle $\mathbf{D}(\mathbf{p}, r) \subset \mathbf{A}$ is called an empty or inscribed circle of the figure $\mathbf{A}$. A maximal empty cir-

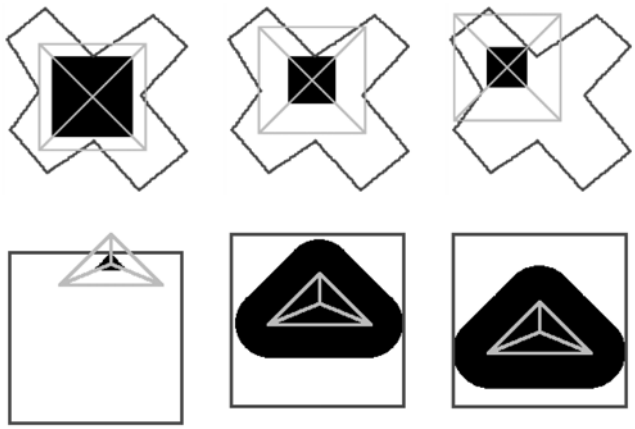

Fig. 2. Projection on shapes of expansion/contraction class.

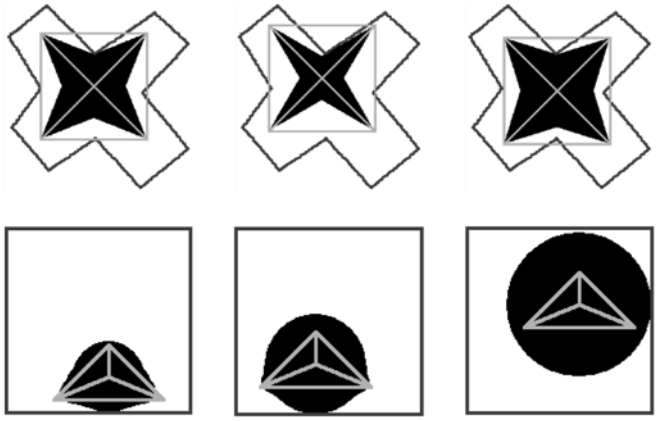

Fig. 3. Projection on shapes of thinning/thickening class.

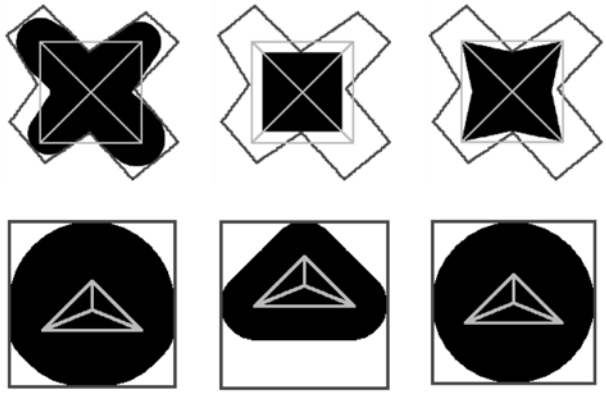

Fig. 4. Invariant projections on shapes of various classes.

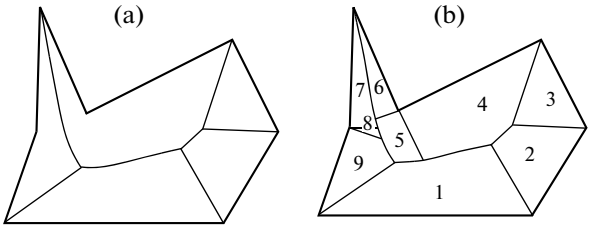

Fig. 5. (a) Polygon skeleton (marked by the red line); (b) Voronoi cells of polygonal figure (indicated by numbers), beginning and end of parabolic bisector are marked by green lines passing through corresponding site.

cle is an empty circle that is entirely contained in no other empty circle of a given figure. The skeleton **S(A)** of figure **A** is a set of centers of all maximal empty circles of the figure. For figure **A**, the radial or distant function of the point $\mathbf{p} \in \mathbf{P}$ is the maximal radius of an empty circle with its center at the point

$$r_{\mathbf{A}}(\mathbf{p}) = \{-\infty: \mathbf{p} \in \mathbf{A}^{\mathbf{C}}; 0: \mathbf{p} \in \partial\mathbf{A};$$

$$\arg\max_{r \in \mathbf{R}}\{\|\mathbf{D}(\mathbf{p}, r)\|: \mathbf{D}(\mathbf{p}, r) \subset \mathbf{A}\}: \mathbf{p} \in \mathbf{A}\}.$$

A Skeleton representation of the figure is the combination of its skeleton and the radial function determined in skeleton points as follows:

$$\mathbf{SR(A)} = \{\langle \mathbf{p}, r_{\mathbf{A}}(\mathbf{p})\rangle: \mathbf{p} \in \mathbf{S(A)}\}.$$

The reconstruction of the figure based on the skeletal representation duplicates the figure as follows:

$$\delta\mathbf{SR(A)} = \cup_{\langle \mathbf{p}, r\rangle \in \mathbf{SR(A)}}\{\mathbf{D}(\mathbf{p}, r)\} = \mathbf{A}.$$

Thus, the introduced elements of the continuous binary morphology are identical with the above-introduced elements of the general monotonic binary morphology. However, in this case, figure skeletons are continuous connected planar graphs, as shown in [4]. Moreover, for figures restricted by polygons with a finite number of sides, the skeleton is proved to involve a finite number of segments of analytic curves of two shapes, i.e., straight and parabolic. Therefore, there are computationally efficient algorithms [4] for constructing continuous skeletons based on generalized Voronoi diagrams.

A classical Voronoi diagram for a given two-dimensional point set **A** is defined as a piecewise linear graph determining the partition of a plane into closed nonintersecting Voronoi cells (sets of points) $\mathbf{T}_i$, each of which includes all plane points for which the same point $\mathbf{p}_i$ is the closest point of the set **A** in terms of a given metric d:

$$\mathbf{T}_i = \{\mathbf{p}: \mathbf{p} \in \mathbf{P}, \mathbf{p}_i \in \mathbf{A},$$

$$\forall \mathbf{p}_j \in \mathbf{A}, \mathbf{p}_j \neq \mathbf{p}_i, d(\mathbf{p}_i, \mathbf{p}) < d(\mathbf{p}_j, \mathbf{p})\}.$$

For the cell $\mathbf{T}_i$, the corresponding point $\mathbf{p}_i$ is the center of the attraction or site.

In the case of a generalized Voronoi diagram, not only isolated points, but also figures (sets of points), for example, continuous segments of boundary lines, can be considered as sites, i.e., centers of attraction. In particular, the boundary of a polygonal figure is represented in the shape of a cyclically ordered set of sites of two types: point sites and segment sites. Point and segment sites with nonempty intersections are called neighboring sites. The point site is the closest site for a point **p** if it is the closest point of the boundary $\partial\mathbf{A}$ to the point **p**. The segment site is the closest site for a point **p** if it involves the closest point of the boundary $\partial\mathbf{A}$ to the point **p**, this closest point being the orthogonal projection of the point **p** on the strain line containing this site. A Voronoi cell for a given boundary site is a set of plane points for which this site is the closest.

Sites are called adjacent if their Voronoi cells have a common nondegenerate boundary (more than one common point). A bisector of two sites is a line with a common boundary of cells of two adjacent sites. The Voronoi diagram **V(A)** of the polygonal figure **A** is the integration of bisectors of all the figure sites.

As is shown in [4], the skeleton of the polygonal figure is the subset of the figure's Voronoi diagram as follows: $\mathbf{S(A)} \subset \mathbf{V(A)}$. Note that the skeleton involves only bisectors of non-neighboring sites. An example of the skeleton and the Voronoi diagram are shown in Fig. 5.

On the other hand, it is also noted in [4] that, in the continuous case, the figure skeleton can be defined as a set of singular points (derivative discontinuity) of the distant function $r_{\mathbf{A}}(\mathbf{p})$. It is easy to verify that, in the case of a polygonal figure, the function $r_{\mathbf{A}}(\mathbf{p})$ is continuous within cells of the Voronoi diagram. Moreover, with centers of attraction (sites) that take the shape of straight-line segments and points, the two-dimensional function $r_{\mathbf{A}}(\mathbf{p})$ within corresponding Voronoi cells is uniquely described by equations of inclined planes (for segment sites) and cones (distance to point sites). Thus, the piecewise smooth distant function $r_{\mathbf{A}}(\mathbf{p})$ can be considered as known as soon as the Voronoi diagram of the polygonal figure **V(A)** is calculated.

Now, let there be given two different continuous binary figures **A** and **B**. According to (2), the morphological projection of the figure **B** on the shape of the figure **A** can be determined by the following expression:

$$\Pr(\mathbf{B}, \mathbf{A}) = \cup_{\mathbf{p} \in \mathbf{S(A)}}\{\mathbf{D}(\mathbf{p}, r_{\mathbf{B}}(\mathbf{p}))\}.$$

It should be noted that the radial function can also take negative values in arbitrary points (if these points do not belong to the figure **B**) and if so $\mathbf{D}(\mathbf{p}, r)$ becomes an empty set. The projection skeleton involves no such points. In addition, with the shape of the function $r_{\mathbf{B}}(\mathbf{p})$ by no means related to the skeleton shape **S(A)**, there may exist points $\mathbf{p}, \mathbf{q} \in \mathbf{S(A)}$ for which $\mathbf{D}(\mathbf{q}, r_{\mathbf{B}}(\mathbf{q})) \subseteq \mathbf{D}(\mathbf{p}, r_{\mathbf{B}}(\mathbf{p}))$.

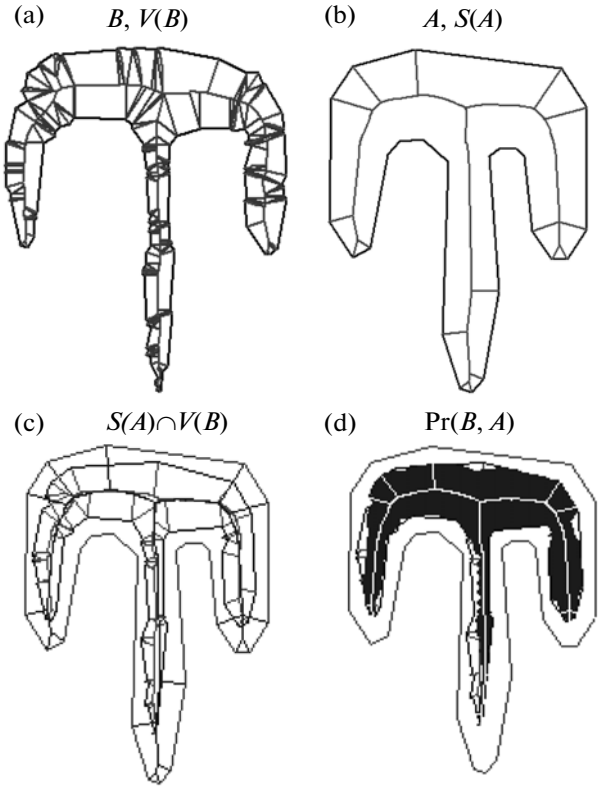

Fig. 6. Projection Pr(**B**, **A**) of figure **B** on shape of figure **A** (projection result is marked in blue).

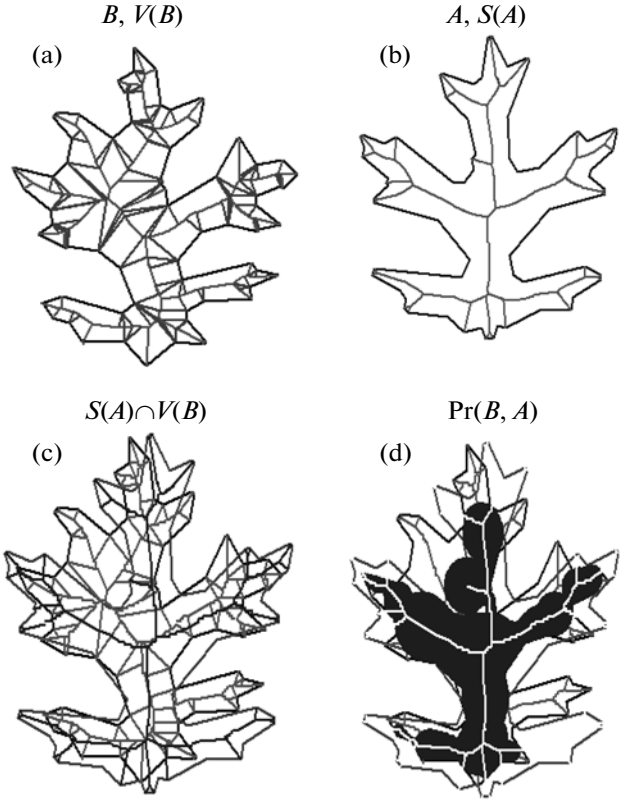

Fig. 7. Projection Pr(**B**, **A**) of figure **B** on shape of figure **A** (projection result is marked in blue).

These pairs of points satisfy the following simple geometric condition:

$$\mathbf{D}(\mathbf{q}, r_{\mathbf{B}}(\mathbf{q})) \subseteq \mathbf{D}(\mathbf{p}, r_{\mathbf{B}}(\mathbf{p})) \Leftrightarrow d(\mathbf{p}, \mathbf{q}) < r_{\mathbf{B}}(\mathbf{p}) - r_{\mathbf{B}}(\mathbf{q}).$$

Hence, it follows that the minimal descriptor of the projection shape is

$$\mathrm{Pr}(\mathbf{B}, \mathbf{A}) = \cup_{\mathbf{p} \in \mathbf{S(A)}} \{\mathbf{D}(\mathbf{p}, r_{\mathbf{B}}(\mathbf{p})): r_{\mathbf{B}}(\mathbf{p}) > 0, \forall \mathbf{q} \in \mathbf{S(A)}, d(\mathbf{p}, \mathbf{q}) > r_{\mathbf{B}}(\mathbf{p}) - r_{\mathbf{B}}(\mathbf{q})\}. \quad (10)$$

Thus, an algorithm for calculating the projection of the figure **B** on the shape of the figure **A** is as follows:

1) construct the Voronoi diagram **V(A)** and the figure skeleton **S(A)**;

2) construct the Voronoi diagram **V(B)**;

3) determine segments of the intersection of the skeleton **S(A)** with cells of the Voronoi diagram **V(B)**;

4) calculate values of the function $r_{\mathbf{B}}(\mathbf{p})$ for obtained segments of the skeleton **S(A)**;

5) reconstruct Pr(**B**, **A**) according to (10).

The algorithm possesses adequate computational efficiency to find use in practice.

Examples of constructing the projection of the figure **B** in the shape of figure **A** are given in Figs. 6 and 7.

CONCLUSIONS

In conclusion, it can be noted that, from an algorithmic point of view, many of the described procedures of morphological projection may be placed into a histogram class, since they are based on analyzing the empiric function of distributing distances from skeleton points of the figure **A** to boundary points of the figure **B**. This function of the shape

$$h_{\mathbf{BA}}(r) = \min_{\mathbf{p} \in \mathbf{S(A)}} \{r_{\mathbf{B}}(\mathbf{p}): r_{\mathbf{A}}(\mathbf{p}) = r\}, \quad (11)$$

which is determined on the set $\mathbf{R} = \cup_{\mathbf{p} \in \mathbf{S(A)}} r_{\mathbf{A}}(\mathbf{p})$, can be called the projection histogram of two figures $\langle \mathbf{B}, \mathbf{A} \rangle$. This histogram contains all necessary data for forming the mapping law (look-up-function) f (7) for any given class of functions F.

Also note that various local restrictions imposed on relationships between radial function values only at individual neighboring skeleton edges can be considered along with global restrictions of shape (7), which are calculated using histograms (11). Apparently, each restriction of this kind defines its own specific morphological system.

ACKNOWLEDGMENTS

This work was supported by the Russian Foundation for Basic Research, project no. 09-07-13551-ofits.

REFERENCES

1. Yu. V. Vizilter and S. Yu. Zheltov, "Comparison and Localization of Image Fragments by Using the Projective Morphologies," Vestn. Komp'yut. Inf. Tekhnol., No. 2, 14–22 (2008).
2. Yu. P. Pyt'ev, "Problems on Image Morphological Analysis," in *Mathematical Methods for Researching the Earth Resources from the Space* (Nauka, Moscow, 1984), pp. 41–83 [in Russian].
3. J. Serra, *Image Analysis and Mathematical Morphology* (Acad. Press, London, 1982).
4. L. M. Mestetskii, *Continuous Morphology of Binary Images: Figures, Skeletons, Circulars* (Fizmatlit, Moscow, 2009) [in Russian].

Yurii Valentinovich Vizilter. Born February 7, 1970 in Moscow. Graduated from the Ordzhonikidze Aviation Institute, Moscow in 1992. Received candidate's degree in 1997 and doctoral degree in 2009. Presently acts as the Head of the Laboratory of Computer Vision of State Scientific Research Institute of Aviation Systems.

Author of more than 70 papers (of which more than 20 papers were published in reviewed VAK journals). Scientific interests: processing and analysis of images, digital photogrammetry, computer vision, mathematical morphology, pattern recognition, machine learning, and biometry. Member of the editorial board of the *Journal of Computer and Information Technology.*

Aleksei Yur'evich Rubis. Born May 13, 1986 in Dedovsk. Graduated from the Moscow Aviation Institute in 2009. Currently a second year postgraduate student and engineer in the Laboratory of Computer Vision of State Scientific Research Institute of Aviation Systems. Author of two papers in *Questions of Defense Technology* (included in the VAK list). Scientific interests: image processing and analysis, computer vision, mathematical morphology, and pattern recognition.

Sergei Vladimirovich Sidyakin. Born December 5, 1985, in Krasnogorsk. Graduated from the Moscow Aviation Institute in 2009. Currently a second year postgraduate student and engineer in the Laboratory of Computer Vision of State Scientific Research Institute of Aviation Systems. Author of two papers in the *Questions of Defense Technology* (included in the VAK list). Scientific interests: processing and analysis of images, computer vision, mathematical morphology, and pattern recognition.

Vladimir Sergeevich Gorbatsevich. Born November 29, 1985 in Kaliningrad. Graduated from Moscow Aviation Institute in 2009. Engineer at the Laboratory of Computer Vision of the State Scientific Research Institute of Aviation Systems. Author of six papers, five of which were published in reviewed VAK journals. Scientific interests: computer vision, image processing, digital photogrammetry, pattern recognition, mathematical morphology, and mobile object control.